SRR-CWDA-2021-00031
Revision 1

Closure Cap Model Parameter Evaluation: Saturated Hydraulic Conductivity of Sand

May 2021

Prepared by: Savannah River Remediation LLC
Waste Disposal Authority
Aiken, SC 29808

Prepared for U.S. Department of Energy Under Contract No. DE-AC09-09SR22505

APPROVALS

Author:

Steven Hommel

Digitally signed by Steven Hommel
Date: 2021.05.24 10:36:34 -04'00'

Steven P. Hommel
WDA Assessments
Savannah River Remediation, LLC

Date

Technical Review per S4-ENG.51:

t9415

Digitally signed by t9415
Date: 2021.05.24 11:11:39 -04'00'

Gregory P. Flach
WDA Assessments
Savannah River Remediation, LLC

Date

Management Review:

KENT H. ROSENBERGER

Digitally signed by KENT H. ROSENBERGER
Date: 2021.05.24 11:17:22 -04'00'

Kent H. Rosenberger
WDA Assessments, Manager
Savannah River Remediation, LLC

Date

REVISION HISTORY

Rev. #	Date	Description
0	March 2021	Initial issue.
1	May 2021	Changed recommended mode in Table 4.3-2 and updated results after consultation with NRC staff.

TABLE OF CONTENTS

LIST OF FIGURES

LIST OF TABLES

ACRONYMS/ABBREVIATIONS

FTF	F-Area Tank Farm
GCL	Geosynthetic Clay Liner
HDPE	High Density Polyethylene
HELP	Hydrologic Evaluation of Landfill Performance Model
K_h	Horizontal Saturated Hydraulic Conductivity
K_{sat}	Saturated Hydraulic Conductivity
K_v	Vertical Saturated Hydraulic Conductivity
LLDL	Lower Lateral Drainage Layer
NRC	Nuclear Regulatory Commission
PNNL	Pacific Northwest National Laboratory
REPM	Relative Effective Porosity Model
RSI	Request for Supplemental Information
SDF	Saltstone Disposal Facility
SDMP	Site Decommissioning Management Plan
SDU	Saltstone Disposal Unit
SPF	Saltstone Production Facility
SRS	Savannah River Site
ULDL	Upper Lateral Drainage Layer
USCS	Unified Soil Classification System
USDA	United States Department of Agriculture

This page intentionally left blank.

1.0 INTRODUCTION

Disposal of salt solution at the Savannah River Site (SRS) began in June of 1990 with very low activity liquid waste and has continued until present day. Salt solution is processed via the Saltstone Production Facility (SPF) into a grout slurry, which is then pumped into Saltstone Disposal Units (SDUs) at the Saltstone Disposal Facility (SDF) where it cures (or hardens) into the final waste form called saltstone. The SDUs currently containing saltstone are SDUs 1, 2A, 2B, 3A, 4, 5A, 5B, and 6. [SRR-CWDA-2019-00110] Note that historically SDUs 1 and 4 have also been referred to as Vaults 1 and 4.

In support of continued waste disposal operations at the SDF, additional SDUs will be constructed and filled with saltstone. [SRR-LWP-2009-00001] Once disposal operations end, the facility will be prepared for permanent closure. [SRR-CWDA-2020-00005]

The *Closure Plan for the Z-Area Saltstone Disposal Facility* (SRR-CWDA-2020-00005) indicates that an engineered closure cap will be installed over the SDF. This closure cap will consist of (from the top-down) a top soil layer, an upper backfill layer, an erosion barrier layer, a geotextile fabric, a middle backfill layer, a geotextile fabric, an upper lateral drainage layer, a geotextile fabric, a high density polyethylene (HDPE) geomembrane, a geosynthetic clay liner (GCL). These materials will be placed over a foundation layer (backfill with bentonite admix). Additional materials placed beneath these layers (i.e.,., a lower backfill layer, a geotextile filter fabric, and a lower lateral drainage layer) are not explicitly included in closure cap modeling as these materials are simulated as part of vadose zone modeling in the *Performance Assessment for the Saltstone Disposal Facility at the Savannah River Site* (SRR-CWDA-2019-00001), hereafter referred to as the 2019 SDF PA.

The performance of the closure cap was evaluated as part of the 2019 SDF PA. After issuing the 2019 SDF PA, the United States Nuclear Regulatory Commission (NRC) issued a letter (ML20254A003), hereafter referred to as the NRC Letter, which includes requests for supplemental information (RSIs) to support their review of the 2019 SDF PA. This report provides some of the requested supplemental information.

1.1 Purpose

The NRC Letter (ML20254A003) indicated that in order to:

> "evaluate the risk significance and the projected performance of the sand drainage layers, the NRC staff needs supplemental information about the uncertainty associated with the [lower lateral drainage layer] LLDL and the upper lateral drainage layer (ULDL)."

The NRC Letter also proposed the following as a path forward:

> "Provide ranges of saturated vertical and horizontal hydraulic conductivity for the sand drainage layers (i.e., both LLDL and ULDL) that reflect the sources of parametric and model uncertainty … The response should address both initial and degraded values. Provide infiltration rates that result from considering those sources of degradation and uncertainty in the ULDL."

Within the NRC Letter (ML20254A003), this RSI is explicitly identified as "RSI-2: Sand Drainage Layers."

The purpose of this report is to partially address RSI-2. This report includes an evaluation of the saturated hydraulic conductivity (K_{sat}) of sands to be used for the sand drainage layers of the closure cap, including considerations for the ranges of potential variability or uncertainty associated with initial conditions and potentially degraded conditions which may affect the long-term performance of the barrier system. Recommendations within this report will be used to construct a probabilistic system model to assess the parametric uncertainty of the model inputs used to estimate the rate of infiltration through the closure cap.

This report does not provide updated infiltration rates, as the cumulative impact of potential changes to the infiltration rates will be evaluated after other RSIs within the NRC Letter (ML20254A003) have been addressed.

1.2 Closure Cap Overview

The layers of the current closure cap conceptual design are based on *Saltstone Disposal Facility Closure Cap Concept Update for Large-Scale Disposal Units* (WSRC-STI-2008-00244), but with an increased slope at the surface (i.e., 3% slope instead of 1.5% slope) to meet closure requirements specified in the *New Consolidated Solid Waste Landfill Regulation*. [SCDHEC R.61-107.19] The closure cap design is preliminary; however, it provides sufficient information for planning, evaluating the closure cap configuration relative to its constructability and functionality, and estimating infiltration rates over time through modeling.

The SDF closure cap is primarily intended to provide physical stabilization of the site, minimize infiltration, and provide an intruder deterrent. Although they are collectively referred to as a single feature due to the similarity in design, two distinct closure caps are anticipated to be constructed over the SDUs at the end of the operational period: one large closure cap for the cylindrical SDUs and one smaller closure cap for the rectangular SDUs (see Figure 1.2-1). Cross sections from this conceptual closure cap design are also provided (see Figure 1.2-2 and Figure 1.2-3). [SRR-CWDA-2018-00087]

Table 1.2-1 identifies each of the SDF closure cap layers and their anticipated thicknesses and are graphically depicted in Figure 1.2-4.

Figure 1.2-1: SDF Closure Cap Conceptual Design Configuration (Plan View)

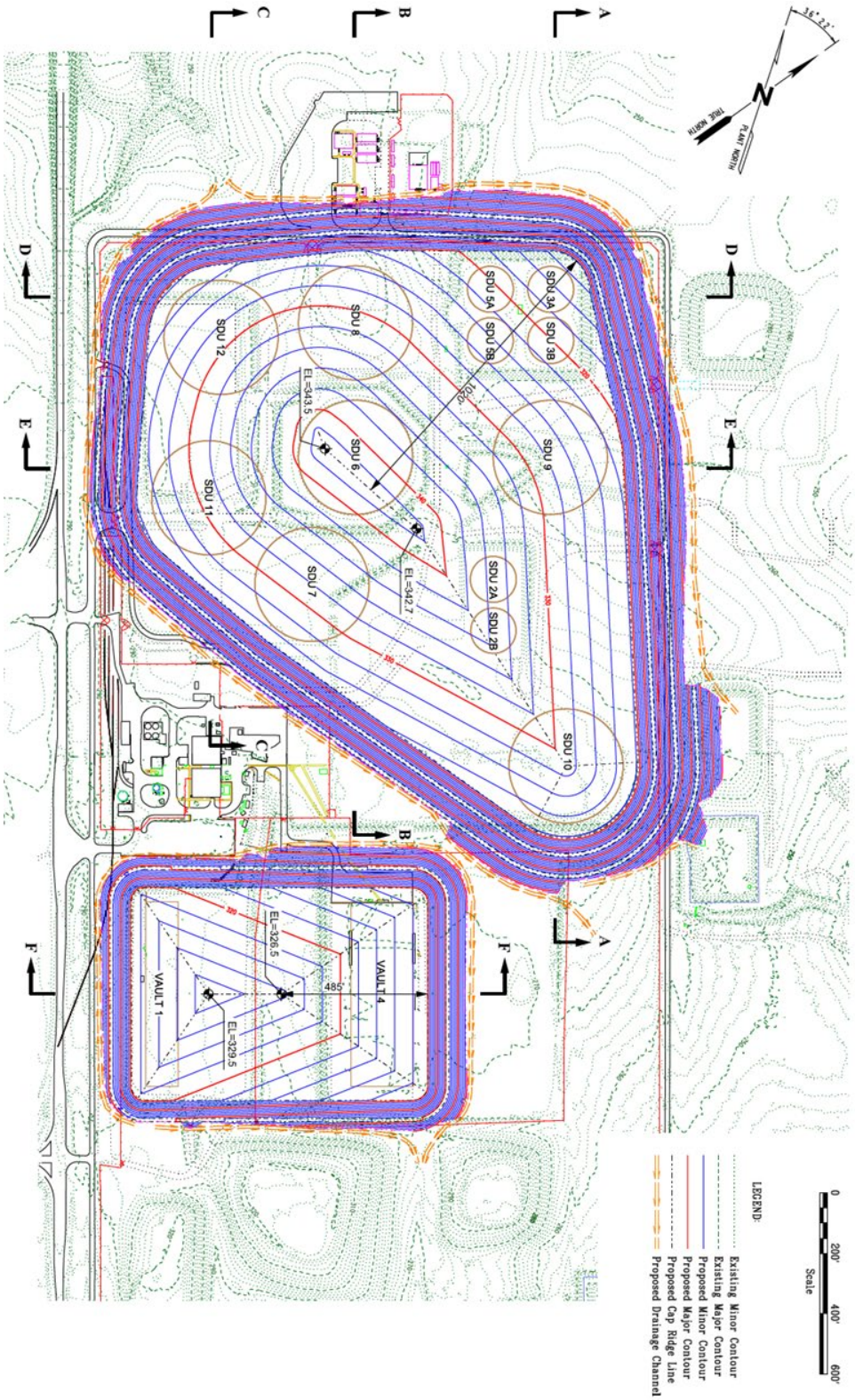

[SRR-CWDA-2018-00087]

Figure 1.2-2: SDF Closure Cap Conceptual Design Configuration (Cross Sections 1 of 2)

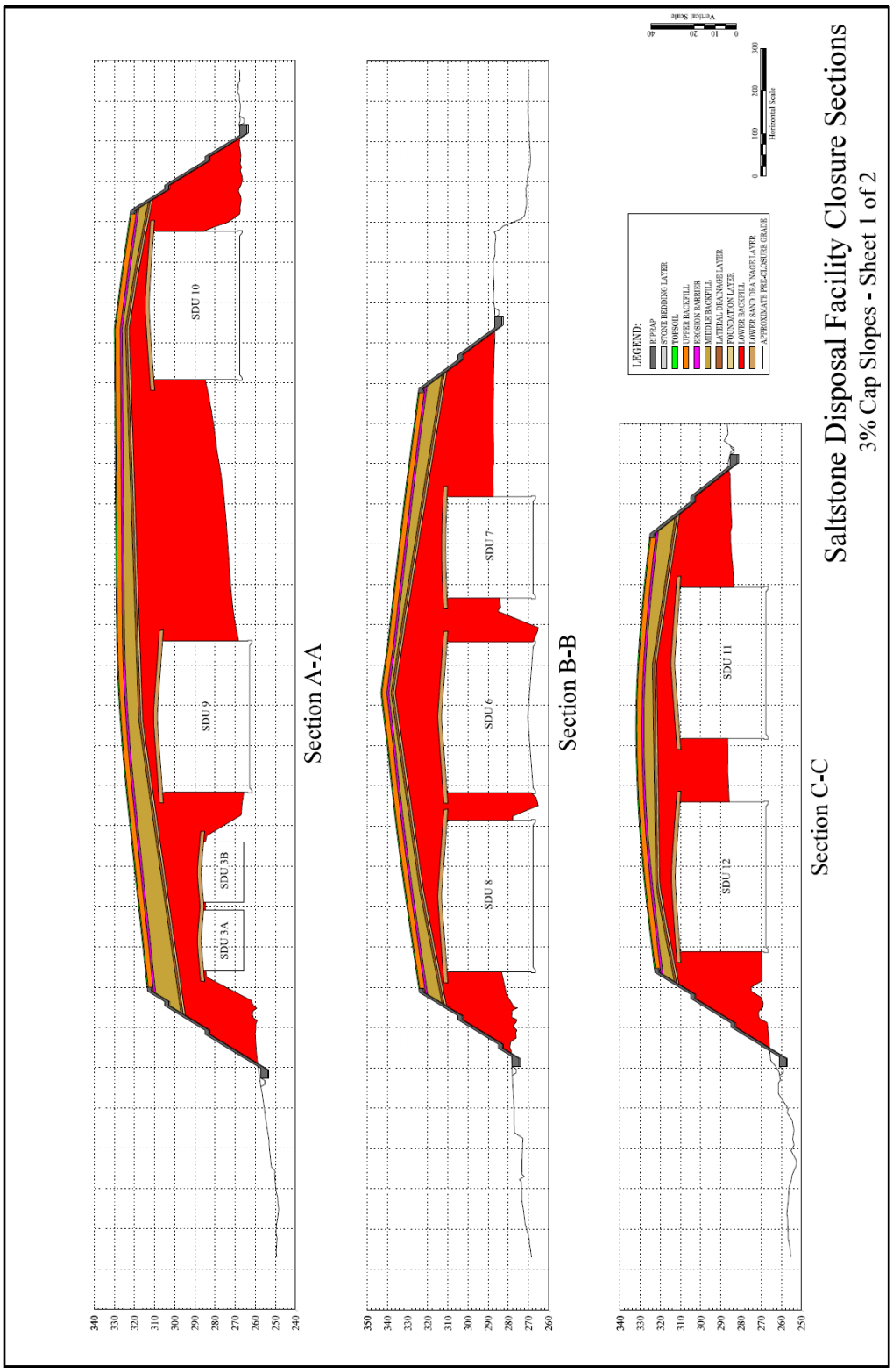

[SRR-CWDA-2018-00087]

Figure 1.2-3: SDF Closure Cap Conceptual Design Configuration (Cross Sections 2 of 2)

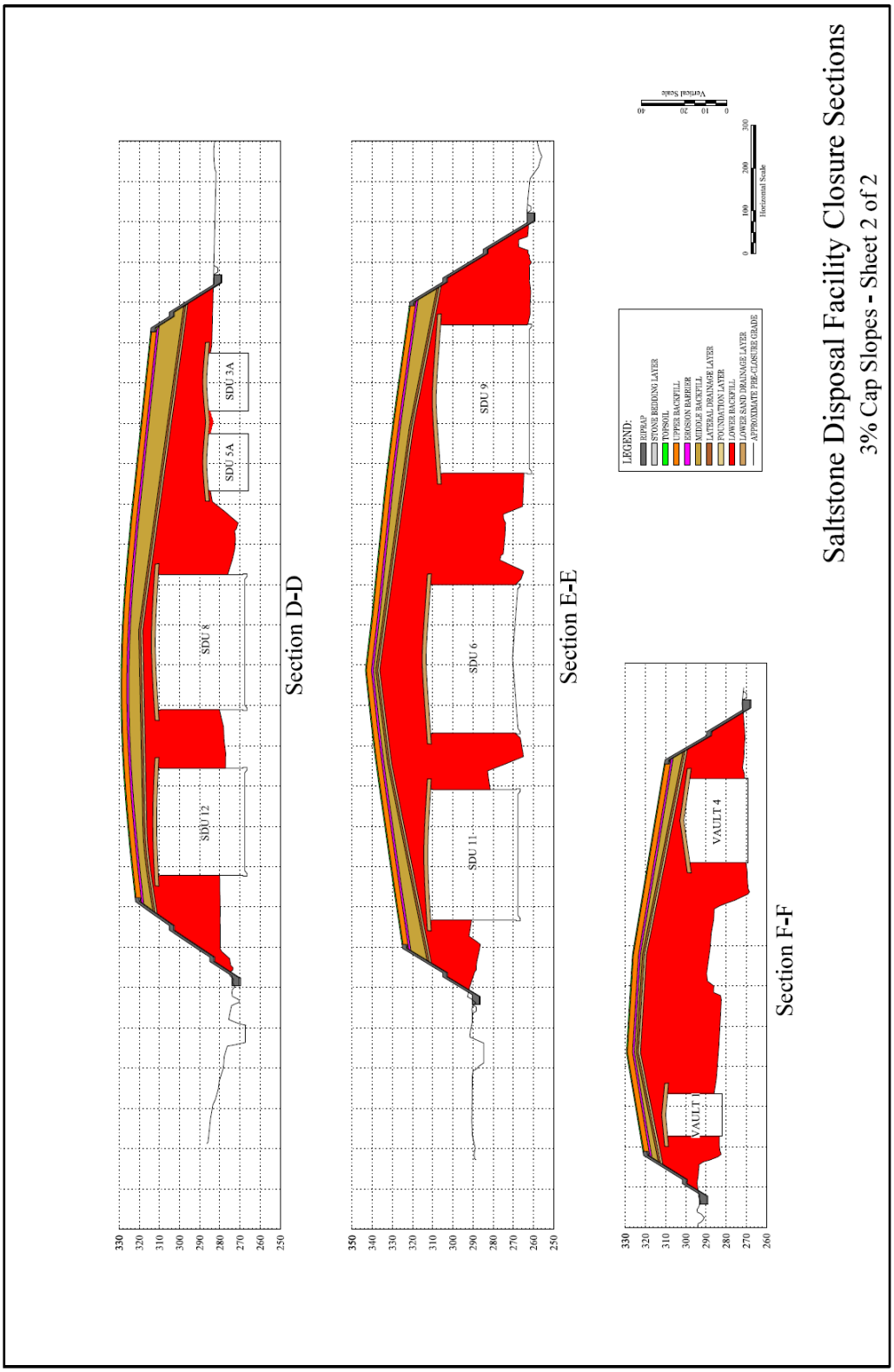

[SRR-CWDA-2018-00087]

Table 1.2-1: SDF Closure Cap Layers and Layer Thicknesses

Layer [a]	Layer Thickness (in)
Vegetative Cover	N/A
Topsoil	6
Upper Backfill	30
Erosion Barrier	12
Geotextile Fabric	Not specified.
Middle Backfill	12 (minimum, will increase from cap apex to toe due to difference between surface slope and the slope of the upper lateral sand drainage layer)
Geotextile Filter Fabric	0.1 (minimum)
Upper Lateral Sand Drainage Layer	12
Geotextile Fabric	Not specified.
High Density Polyethylene (HDPE) Geomembrane	0.06 (60 mil)
Geosynthetic Clay Liner (GCL)	0.2
Foundation Layer (backfill with bentonite admix) [b]	12
Lower Backfill [b]	12 (minimum, will increase from cap toe to apex due to slope of the upper lateral sand drainage layer)
Geotextile Filter Fabric [b,c]	Not specified.
Lower Lateral Sand Drainage Layer, extends approximately 25 feet from disposal unit [b,c]	24
Geotextile Fabric [b,c]	Not specified.
HDPE Geomembrane [b,c]	0.1
GCL [b,c]	0.2

[WSRC-STI-2008-00244, Table 4 and SRR-CWDA-2018-00087 (Attachments)]
(a) The layers are arranged in the table to reflect their order from top to bottom in the SDF closure cap.
(b) Layer is not included in closure cap modeling.
(c) Layer is above each disposal unit and does not cover the entire SDF area.

Figure 1.2-4: SDF Conceptual Closure Cap Layers

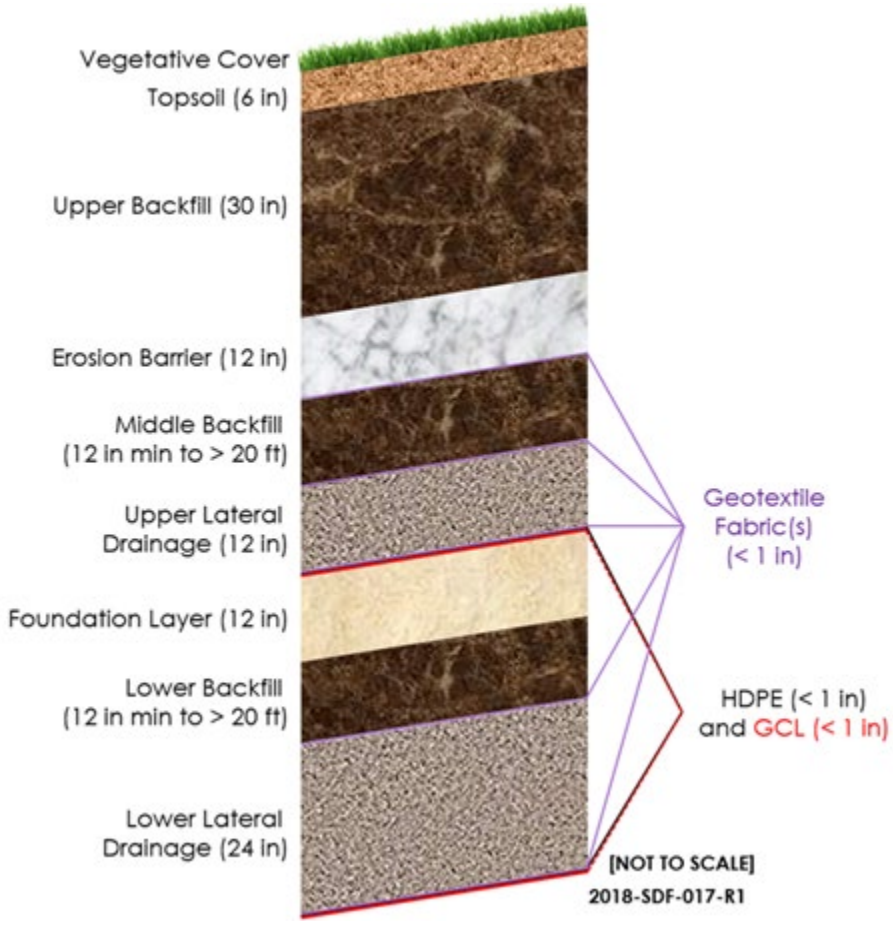

[SRR-CWDA-2018-00006]

Table 1.2-2 provides the approximate closure cap thicknesses over each SDU. The average lower backfill thicknesses come from Table 7.1-1 of SRR-CWDA-2018-00068, wherein the values were estimated by examining the cross sections shown in Figure 1.2-2 and Figure 1.2-3. The approximate closure cap thickness is then estimated as the sum of:

- the lower lateral drainage layer thickness (2 ft),
- the average backfill thickness (varies by SDU),
- the foundation layer thickness (1 ft),
- the upper lateral drainage layer thickness (1 ft),
- the middle backfill layer (assumed to be 1 ft, based on the minimum thickness),
- the erosion barrier thickness (1 ft),
- the upper backfill thickness (2.5 ft), and
- the topsoil thickness (0.5 ft).

This estimate gives no credit to HDPE, GCL, or geotextile fabrics. The minimum closure cap thickness was estimated to be approximately 14 feet (over SDUs 1 and 4) and the maximum closure cap thickness was nearly 30 feet (over SDUs 2A and 2B).

Table 1.2-2: Approximate Average Closure Cap Thickness Over Each SDU

SDU	Average Lower Backfill Thickness (ft) Based on Conceptual Closure Cap Design	Approximate Closure Cap Thickness Over SDU (ft)	Approximate Closure Cap Thickness Over SDU (m)
SDU 1	4.9	13.9	4.2
SDU 2A	20.1	29.1	8.9
SDU 2B	20.1	29.1	8.9
SDU 3A	12.6	21.6	6.6
SDU 3B	17.0	26.0	7.9
SDU 4	4.9	13.9	4.2
SDU 5A	18.9	27.9	8.5
SDU 5B	18.9	27.9	8.5
SDU 6	18.7	27.7	8.4
SDU 7	12.0	21.0	6.4
SDU 8	5.5	14.5	4.4
SDU 9	6.7	15.7	4.8
SDU 10	5.6	14.6	4.5
SDU 11	7.1	16.1	4.9
SDU 12	5.3	14.3	4.4

1.3 Upper and Lower Lateral Drainage Layers

The upper and lower lateral drainage layers consist of coarse sands. The upper lateral drainage layer has a minimum thickness of 12 inches and lies directly above an impermeable composite barrier (i.e., HDPE and GCL). The lower lateral drainage layer has a minimum thickness of 24 inches and also lies directly above an impermeable composite barrier.

The reason for using coarse sand, as opposed to medium- or fine-grained sands, is that coarse sand has a higher saturated hydraulic conductivity (K_{sat}), which means that water more readily flows through this material. This layer provides a lateral flow path so that any water that reaches it can shed laterally away, towards the perimeter of the closure cap, and away from underlying SDUs. Materials with a lower K_{sat} would slow down the lateral flow, resulting in greater downward flow towards the SDUs.

2.0 SDF CLOSURE CAP MODELING

Section 4.4.1 of the 2019 SDF PA (SRR-CWDA-2019-00001) describes the SDF Closure Cap Model used to estimate infiltration rates into the vadose zone. This is summarized in Section 2.1.

The SDF closure cap model is organized into two parts: (1) a WinUNSAT-H model used to simulate near-surface conditions and determine the "deep percolation" or "impingement rate" past the root zone, and (2) an analytical solution used to estimate drainage flow and barrier leakage. For the purposes of the 2019 SDF PA, the leakage rate from this analytical solution is used as the infiltration rate into the vadose zone model. Because the lateral drainage layers are not included in the WinUNSAT-H model, this first part of the SDF Closure Cap is not discussed herein. However, the analytical solution is described in Section 2.2.

2.1 Conceptual Approach

Conceptually, the SDF Closure Cap Model is organized into two parts. The first part addresses the percolation through the upper layers of the closure cap down to the upper lateral drainage layer, while the second part considers the leakage rate based on the combined performance of the upper lateral drainage layer and the "composite barrier" (i.e., the combined HDPE and GCL layers). Note that the lower layers (i.e., the foundation layer, the lower backfill layer, the lower lateral sand drainage layer, and the composite barrier (HDPE and GCL layers) directly above each SDU) are not included in the SDF Closure Cap Model. The 2019 SDF PA models do not include the foundation layer, while the other lower layers are all included as part of the Vadose Zone Flow Model (SRR-CWDA-2019-00001).

Figure 2.1-1 shows the conceptual model for the first part of the SDF Closure Cap Model. This part of the model addresses how meteorological/environmental conditions and material properties influence percolation through the root zone to the upper lateral sand drainage layer. As shown, water is introduced into the system as precipitation (P). Solar radiation and vegetation remove water from the system via evaporation (E) and transpiration (T), respectively. Surface runoff (R) also removes water from the system. The remaining water is then expected to percolate downward past the root zone. The rate of percolation (P_r) is then determined based on the hydraulic properties of each layer of the closure cap. Within the 2019 SDF PA, this part of the model estimated a percolation rate of approximately 400 mm/yr. [SRR-CWDA-2019-00001]

Figure 2.1-1: Conceptual Model for Percolation Through the Upper Closure Cap

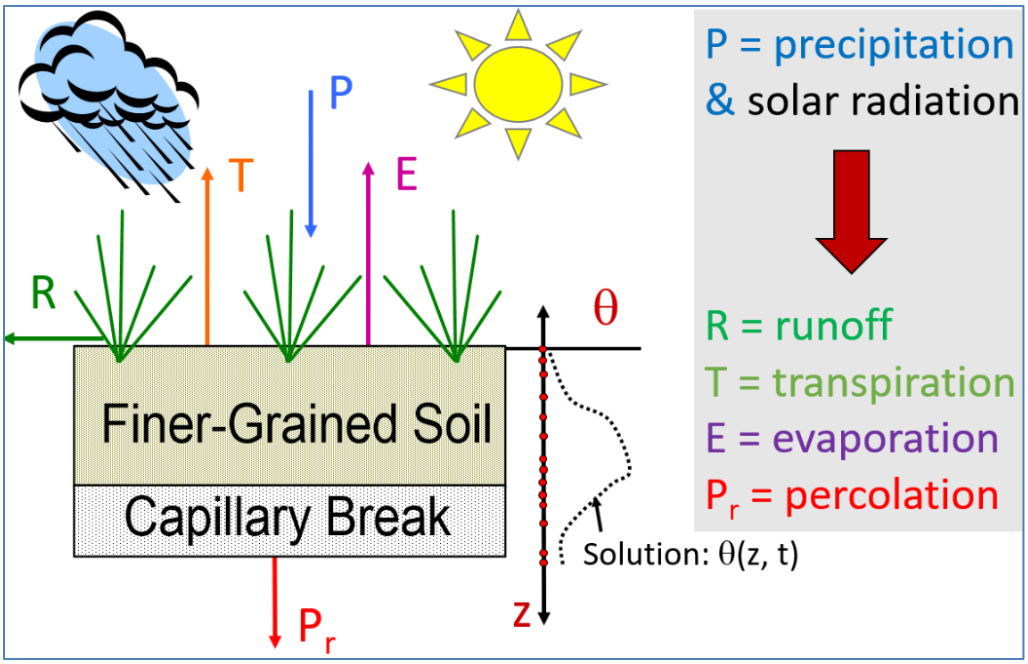

[SRR-CWDA-2018-00035]

Figure 2.1-2 shows the conceptual model for the second part of the SDF Closure Cap Model. Water percolating from above will enter the upper lateral sand drainage layer. Within the sand, downward flow is expected to be significantly impeded by the composite barrier. As such, most of the percolating water is expected to follow the slope of the closure cap and shed laterally to the edges of the SDF closure cap. However, due to assumed holes through the HDPE some of the water will leak through the composite barrier. Infiltration into the lower backfill for the Vadose Zone Model is assumed to be equal to the leakage rate through the composite barrier.

Figure 2.1-2: Conceptual Model for Leakage Through the Composite Barrier

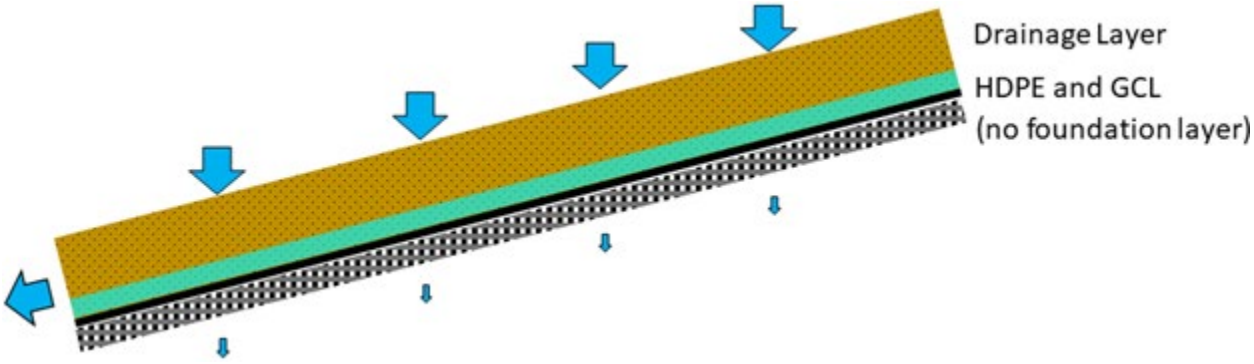

[SRR-CWDA-2018-00035]

2.2 The Giroud-Houlihan Analytical Solution

The leakage rate through the composite barrier is estimated using a semi-empirical formula known as the Giroud-Houlihan analytical solution. This formula was recommended by Benson and Benavides (2018) and was developed based on Giroud (1997) and Giroud, et al. (2004).

This formula estimates the leakage rate (Q) from a single defect in the composite barrier based on an average depth of lateral flow, $qL/K_d sin\beta$:

$$Q = 0.976 C_{qo} \left[1 + 0.1 \left(\frac{qL}{t_b K_d \sin\beta}\right)^{0.95}\right] d^{0.2} \left(\frac{qL}{K_d \sin\beta}\right)^{0.9} K_b^{0.74}$$

where:

Q = leakage rate per HDPE hole (or defect) in m^3/s,

C_{qo} = contact factor (unitless),

q = percolation rate from middle backfill into the upper lateral sand drainage layer in m/s,

L = horizontal slope length in m,

t_b = thickness of the GCL barrier in m,

K_d = hydraulic conductivity of the upper lateral sand drainage layer in m/s,

β = angle in radians, which is effectively the slope (rise over run),

d = diameter of HDPE hole (or defect) in m, and

K_b = hydraulic conductivity in m/s of the GCL barrier.

The K_d value in this equation is the saturated hydraulic conductivity of the sand in the upper lateral drainage layer. This value is discussed further throughout the rest of this report. The other values listed above are discussed in Section 4.4.1 of the 2019 SDF PA (SRR-CWDA-2019-00001) and are not the subject of this report.

This page intentionally left blank.

3.0 INITIAL SAND K_{sat} VALUES

For the SDF closure cap modeling used in the 2019 SDF PA (SRR-CWDA-2019-00001), and summarized in Section 2.0, the initial sand K_{sat} in the upper lateral drainage layer was assumed to be 5.0E-02 cm/s. This same value was also assumed for the lower lateral drainage layer. Section 3.1 describes the basis for this value. Section 3.2 provides an additional evaluation of this value to better reflect the potential uncertainties associated with this parameter.

3.1 Basis of the Initial Sand K_{sat} Assumed for the 2019 SDF PA

Both the upper lateral drainage layer and the lower lateral drainage layer are assumed to have the same initial material properties, including the initial K_{sat} of 5.0E-02 cm/s.

Note that while many of the materials in the 2019 SDF PA were modeled with distinct values for the vertical K_{sat} (or K_v) and for the horizontal K_{sat} (or K_h), the sand material is assumed to be isotropic, that is, has the same values regardless of the flow direction: $K_h = K_v$. When distinct values are applied, as with backfill[1], $K_h > K_v$, indicating that the relationship between the distinct K_{sat} values generally promote greater horizontal (or lateral flow) as opposed to vertical (or downward flow).

The basis for the assumed initial K_{sat} of 5.0E-02 cm/s is provided in Section 5.4.4 of *Saltstone Disposal Facility Closure Cap Concept Update for Large-Scale Disposal Units* (WSRC-STI-2008-00244). Specifically, it states that:

> "[S]and utilized for the lateral drainage layer will be a procured material rather than a material obtained from [an] SRS borrow pit. Therefore, a minimum saturated hydraulic conductivity of the sand will be a requirement in the specification for the procurement of the sand."

Table 14 of WSRC-STI-2008-00244 (reproduced here as Table 3.1-1) lists various K_{sat} values for sands and gravels. The values in this table range from a minimum of 1.0E-04 cm/s (for "Various natural sands" per Lamb and Whitman (1969)) to a maximum of 1 cm/s (for "Clean sand or sand and gravel" per Bear (1972)). The last three rows (unshaded) in the table identify "procured" sands as opposed to the natural sands. These sands range from a low value of 5.0E-02 cm/s to a high value of 4.5E-01 cm/s. Based on this information, a minimum K_{sat} of 5.0E-02 cm/s was specified for the design and is appropriate to use as the initial value for modeling. As such, this is the value used in the 2019 SDF PA (SRR-CWDA-2019-00001).

Note that the material in Table 3.1-1 with the K_{sat} of 5.0E-02 cm/s is identified as "Foster Dixiana FX-50 fine gravel pack" per Phifer, et al. (2001). This material was been identified as having a grain size range of 0.36 mm to 1.75 mm (WSRC-TR-2001-00015). Although the name of this material includes "gravel," the Wentworth (1922) grain size chart classifies this range as medium-grained (0.25 mm to 0.5 mm), to coarse-grained (0.5 mm to 1 mm), to very coarse-grained sand (1 mm to 2 mm). As such, it is appropriate to refer to this material as a coarse sand. In order to meet the design specifications, it is expected that the lateral drainage layers of the closure cap will be constructed using procured sands of similar (or greater) grain sizes.

[1] Table 4.3-2 of the 2019 SDF PA (SRR-CWDA-2019-00001) recommends a K_h = 7.6E-05 cm/s and a K_v = 4.10E-05 cm/s.

To ensure that the minimum K_{sat} of 5.0E-02 cm/s is achieved, it is expected that the material will undergo some degree of processing (e.g., washing and screening), regardless of the source. Such processing will likely result in a relatively uniform material for use in the construction of the lateral drainage layer, with an average K_{sat} that would be notably higher than 5.0E-02 cm/s.

Table 3.1-1: Sand Saturated Hydraulic Conductivities from WSRC-STI-2008-00244

Material	Saturated Hydraulic Conductivity, K_{sat} (cm/s)	Source
SRS water table aquifer at the TNX Terrace	2.1E-02	Phifer et al. 2001 Table 5
Natural deposit of clean sand	<1E-03 to 1	Freeze and Cherry 1979 Table 2.2
Clean sand or sand and gravel	1E-03 to 1	Bear 1972 Table 5.5.1
Various natural sands	1E-04 to 2.0E-01	Lamb and Whitman 1969, Figure 19.5
Sedimentary deposit of well-sorted sand, glacial outwash	1E-03 to 1E-01	Fetter 1988 Table 4.5
Sandy soils	1E-03 to 1E-02	Hillel 1982
HELP[2] model default soil #1 [a]	1E-02	Schroeder et al. 1994 Table 1
Foster Dixiana FX-50 fine gravel pack	5.0E-02	Phifer et al. 2001 Table 7
Foster Dixiana FX-99 coarse gravel pack	4.5E-01	Phifer et al. 2001 Table 7
Fine gravel	1.5E-01	Phifer et al. 2006 Table 5-18 and Yu et al. 1993

Notes: Materials in gray are natural sands and the other items are procured materials.
[a] HELP model default soil #1 is a natural coarse sand (USDA[3]) or poorly graded sand (USCS[4])

3.2 Recommendations for Modeling the Parametric Uncertainty of the Initial Sand K_{sat}

Because a minimum K_{sat} of 5.0E-02 cm/s is specified for the conceptual design of the lateral drainage layers, and product variability will be accounted for during construction, higher values are expected, on average, such that the conceptual design specification will be met or exceeded.

This type of uncertainty is discussed within a NUREG prepared by Pacific Northwest National Laboratory (PNNL) for the NRC, *Uncertainty Analyses of Infiltration and Subsurface Flow and Transport for SDMP [5]Sites* (NUREG/CR-6565). Within that report, recommended probability distributions were developed for various hydraulic soil parameters based on the textures of the soils. For generic sands, Table A-1 of NUREG/CR-6565 recommends applying a truncated beta distribution with a mean of 8.22E-03 cm/s, a standard deviation of 4.39E-03 cm/s, a minimum of 3.50E-04 cm/s, and a maximum of 1.86E-02 cm/s. These values are all lower than the conceptual design minimum of 5.0E-02 cm/s. This is because the generic "sand" described in NUREG/CR-6565 is not representative of the coarse-grained and washed sands that will be used in the lateral drainage layers.

[2] HELP = Hydrologic Evaluation of Landfill Performance Model
[3] USDA = United States Department of Agriculture
[4] USCS = Unified Soil Classification System
[5] SDMP = Site Decommissioning Management Plan

For additional perspective on the differences between fine-grained, medium-grained, and coarse-grained sands, Hwang, et al. (2017) published a comparison of three sets of sands (fine, medium, and coarse) and using three different techniques for estimating the K_{sat} values.

The grain sizes studied by Hwang, et al. (2017) were binned based on sieving mesh sizes, where:

- 0.5 mm to 1 mm for coarse-grained sand,
- 0.25 mm to 0.5 mm for medium-grained sand, and
- 0.125 mm to 0.25 mm for fine-grained sand

The three K_{sat}-estimating techniques compared by Hwang, et al. (2017) were:

- empirical methods,
- breakthrough curve analyses, and
- the relative effective porosity model (REPM)

Hwang, et al. (2017) showed a comparison of the estimated K_{sat} values, reproduced here as Figure 3.2-1. Note that the scale shown by Hwang, et al. (2017) is in cm/min as opposed to cm/s.

Figure 3.2-1: Comparison of Saturated Hydraulic Conductivities Estimated in Hwang, et al. (2017)

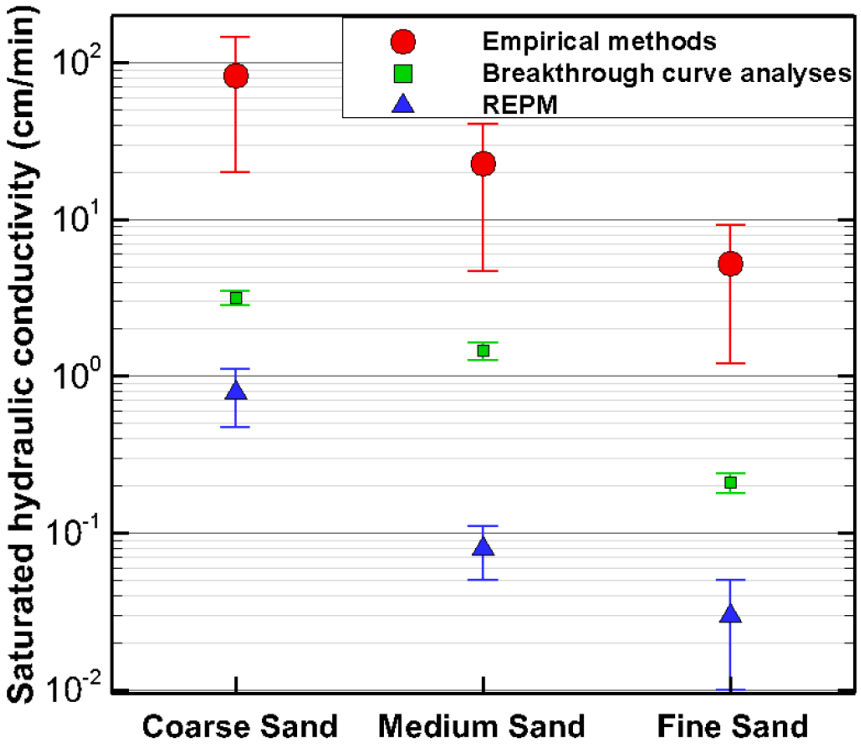

Table 3.2-1 provides the mean values, converted from cm/min to cm/s. While the measurement techniques show significant variability, the relative difference between the different sands were fairly consistent. The K_{sat} values for the coarse grain sands were approximately 2.2 to 8.6 times

higher than the medium grain sands, and approximately 14 to 23 times higher than the fine grain sands.

Table 3.2-1: Sand Saturated Hydraulic Conductivities from Hwang, et al. (2017)

Estimation Method	Coarse Sand K_{sat} (cm/s)	Medium Sand K_{sat} (cm/s)	Fine Sand K_{sat} (cm/s)
Empirical Method[a]	1.29E+00	3.50E-01	9.16E-02
Breakthrough Curve Analysis, mean	5.30E-02	2.42E-02	3.50E-03
REPM, mean	1.15E-02	1.33E-03	5.00E-04

Notes: [a] Hwang, et al. (2017) did not explicitly provide mean values for the Empirical Method; instead, the values shown here are the means of the minimum and maximum values from Hwang, et al. (2017).

The mean of the breakthrough curve estimate for the coarse sand (5.30E-02 cm/s) is very close to the initial value of 5.0E-02 cm/s assumed in the SDF PA. The mean value for the generic sands (8.22E-03 cm/s), as recommended in Table A-1 of NUREG/CR-6565, is approximately midway between the mean K_{sat} values for the medium and fine sands from the breakthrough curve estimates. This suggests that the distributions recommended from NUREG/CR-6565 are skewed towards finer grained materials and would not be appropriate to apply to coarse grained sands.

Based on the observations above, a truncated beta distribution will still be assumed, as recommended in Table A-1 of NUREG/CR-6565, but the mean will be the value for "fine gravel" from Table 3.1-1; it is reasonable to assume a mean value that is higher than 5.0E-02 cm/s since 5.0E-02 cm/s is the minimum acceptable value per the conceptual design (so higher values should be more likely). The minimum will be the conceptual design minimum (5.0E-02 cm/s), and the maximum will be the highest sand value from Table 3.2-1 (1.29E+00 cm/s). This provides a range of values that spans more than an order of magnitude.

For the standard deviation, the value of 4.39E-03 cm/s from Table A-1 of NUREG/CR-6565 was scaled up by a factor of 18.25 (to 8.0E-02 cm/s) because the assumed mean of 1.50E-01 cm/s is approximately a factor of 18.25 times higher than the mean recommended for the generic sands (8.22E-03 cm/s from Table A-1 of NUREG/CR-6565). These recommendations are summarized in Table 3.2-2 and Figure 3.2-2 shows the resulting probability density.

It may be noted that the distribution shown in Figure 3.2-2 is skewed with a narrow tail to the right. Because lower K_{sat} values are conservative, this skewed distribution is believed to be conservative.

Table 3.2-2: Recommended Initial Sand K_{sat} Distribution for Modeling Upper and Lower Lateral Sand Drainage Layers

Distribution Parameter	Generic Sand K_{sat} (cm/s) per NUREG/CR-6565	Recommendation for K_{sat} (cm/s) of Sand in the Upper and Lower Lateral Sand Drainage Layers	Basis for Upper and Lower Lateral Sand Drainage Layers Recommendations
Mean	8.22E-03	1.5E-01	Assumed based on the "Fine gravel" value in Table 3.1-1
Standard Deviation	4.39E-03	8.0E-02	Because the assumed mean (1.50E-01 cm/s) is 18.25 times higher than the mean in Table A-1 of NUREG/CR-6565 (8.22E-03 cm/s), the standard deviation was scaled up by the same factor: 4.39E-03 cm/s × 18.25 = 8.0E-02 cm/s
Minimum	3.50E-04	5.0E-02	Minimum specification from WSRC-STI-2008-00244.
Maximum	1.86E-02	1.29E+00	Estimated Empirical Method value for coarse sands from Hwang, et al. (2017) (see Table 3.2-1)
Shape	Beta		Generic Sand Distribution from Table A-1 of NUREG/CR-6565

Figure 3.2-2: Probability Density Function for the Recommended Initial Condition for the K_{sat} of the Upper and Lower Lateral Sand Drainage Layers

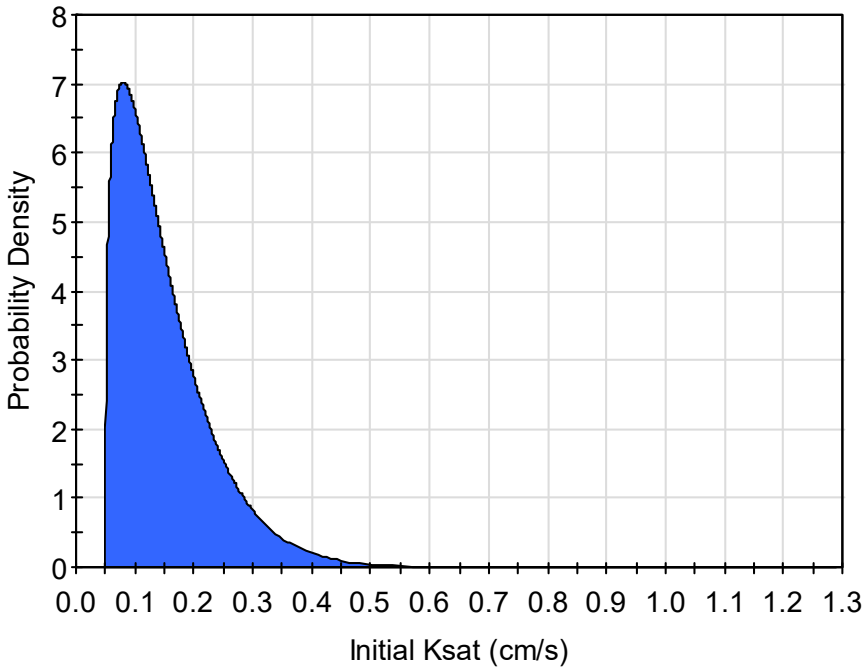

This page intentionally left blank.

4.0 DEGRADATION OF SAND K_{sat} VALUES

As indicated in Section 1.3, higher K_{sat} values increase lateral drainage over the top of the composite barrier and thereby reduce downward leakage towards the SDUs. Alternatively, lower K_{sat} values will increase the downward leakage towards the SDUs. Therefore, the sand material is considered to undergo "degradation" only if the K_{sat} values decrease.

In the 2019 SDF PA (SRR-CWDA-2019-00001), it was generically assumed that at 500 years after closure, the sand K_{sat} would decrease by a factor of 5 as a way to address potential uncertainties associated with the long-term performance of the upper lateral drainage layer. However, there was no technical basis for this factor, so it is appropriate to develop more detailed considerations.

There are three processes which have been postulated as potential degradation mechanisms for the lateral drainage layers: mineral precipitation and microbial growth, root penetrations (for the upper lateral sand drainage layer only), and silting-in (WSRC-STI-2008-00244). None of these processes are expected to occur at a large enough scale to significantly affect the bulk performance of the system; however, enough uncertainty is associated with some of these processes as to warrant additional considerations.

4.1 Mineral Precipitation and Microbial Growth

As previously noted by Jones and Phifer (2008):

> "[D]egradation of sand layers due to mineral precipitation and microbial growth are primarily degradation mechanisms associated with leachate collection layers rather than closure cap lateral drainage layers. Leachate collection layers receive leachate containing both organic and inorganic degradation products from the waste; whereas closure cap lateral drainage layers only receive non-contaminated water from infiltration (in the case of SRS, infiltrating water is very low in both mineral and organic content). Therefore mineral precipitation and microbial growth within the lateral drainage layer is not considered an applicable degradation mechanism" (WSRC-STI-2008-00244).

This means that minerals and microbes typically associated with landfill leachates will not affect the performance of the sand drainage layers.

4.2 Root Penetrations into the Upper Lateral Drainage Layer

In the 2019 SDF PA (SRR-CWDA-2019-00001), it is assumed that the surface of the closure cap will be vegetated by grass. However, it is acknowledged that this grass vegetation will likely be overcome by a succession of pine trees in the long-term. While these pines can have tap roots that may extend more than five to six feet (i.e., into the upper lateral sand drainage layer), or even up to 12 feet, the bulk of the root mass is expected to remain within the topmost 18 inches of the soil based on Brewer (1975).

Tree roots that do extend into the upper sand drainage layer are not expected to penetrate beyond the composite barrier because, as explained by Benson and Benavides (2018):

> "[Roots are] opportunistic, seeking out sources of water that require the least amount of energy to extract. Roots accumulate in regions where water is more plentiful and readily extracted, and do not grow towards regions where water is less plentiful and more difficult

> to extract. For example, when covers are exhumed, roots are observed on the surface of textural contrasts where water accumulates (e.g., on the upper surface of fine-over-coarse arrangement of soil layers)." [SRRA107772-000009]

Roots are expected to grow into regions where water is most plentiful and that will require the least amount of energy for root water uptake. Because the drainage layer will not have readily accessible water, except during short periods following an extended storm event or wet periods in the cooler months. The most plentiful and accessible water will be in the fine textured soil directly above the drainage layer, as a result of the textural contrast between the fine-textured soil and the coarse-textured drainage layer. For this reason, roots normally spread laterally above the drainage layer, and do not penetrate the drainage layer. Per Benson (2021), this is consistent with observations when exhuming final cover profiles. Therefore, the lateral extent of the rooting systems are likely to be most pronounced (1) near the surface and (2) within the finer backfill layers. Moving down through the closure cap layers, it is expected that the density of the root structures will decrease with depth as water becomes less available in each layer.

It should also be noted that pines require more water than grasses, so pine succession would result in increased evapotranspiration relative to the grasses that were assumed for the 2019 SDF PA. This would reduce the amount of water that remains available for deeper infiltration. Accordingly, while root formation within the upper lateral drainage layer may alter the effective K_{sat} of the lateral drainage layer, the combined effects when appropriately considering the dynamic relationships throughout the system are likely to be somewhat offset relative to the overall infiltration estimates.

Regardless of these complex relationships, Section 7.4 and Appendix I of *Saltstone Disposal Facility Closure Cap Concept and Infiltration Estimates* (WSRC-STI-2008-00244) applied a series of assumptions to estimate the potential impacts on the sand K_{sat} due to long-term root growth. From that analysis, the presence of roots was estimated to potentially occupy up to 0.17% of the overall volume of the upper sand drainage layer. However, this volume was estimated to decrease the overall K_{sat} of the sand drainage layer by only 0.2%, as a worst-case assumption. This potential decrease in the K_{sat} is considered negligible relative to other uncertainties in the long-term performance of the system. Therefore, as a conservatism, a root function multiplier of 0.998 (100% – 0.2% = 99.8%) will be applied to the K_{sat} values. This degradation mechanism was not included in the 2019 SDF PA (SRR-CWDA-2019-00001).

4.3 Silting-In

"Silting-in" is a process that assumes that the lateral sand drainage layers will silt-in over time, as fine particles (e.g., colloidal clays) migrate into the coarse sand from the overlying backfill. [WSRC-STI-2008-00244]

4.3.1 Analog Studies Suggesting the Silting-In Will Not Occur

As described in *Predicting Long-Term Percolation from the SDF Closure Cap*, the silting-in phenomenon "has not [been] observed during exhumation of modern final covers or in historic sites that are analogs." [SRRA107772-000009] This can be seen in photographs of the layered soils analogs shown in Figure 4.3-1, Figure 4.3-2, and Figure 4.3-3. These figures show distinct layers between materials with different hydraulic properties. If fine particles were migrating from

the upper layers into the lower layers, the distinctions between the layers would be less pronounced.

Of the three sites depicted, the 3,000-year-old Tu-Dun tombs in south-central China (Figure 4.3-2) is the most geographically and climatologically similar to the Savannah River Site (SRS). This site is located near Jintan in the Jiangsu province of the People's Republic of China. The topography of this region is hilly, like SRS, with average elevations ranging from 10 m to 260 m (30 feet to 850 feet) above mean sea level. [Onitsuka, et al. (2006)] The base elevation of the tombs depicted in Figure 4.3-2 was 50 m (164 feet) above mean sea level. [Onitsuka, et al. (2006)] This compares with the base elevation of the SDF of approximately 260 feet. [SRR-CWDA-2019-00001] The tombs were constructed to be approximately 4.5 m (or 15 feet) above the base elevation. This compares to the minimum closure cap thickness of approximately 4.4 m (14.4 ft) per Table 1.2-2.

Jintan, China has a temperate climate with the average rainfall of 1063.5 mm/yr (42 in/yr) and an average annual temperature of 15.3 °C (59.5 °F) (per Wikipedia article: https://en.wikipedia.org/wiki/Jintan_District). These values compare to SRS with an average annual rainfall of approximately 49 in/yr and average annual temperature of approximately 64.4 °F (per Tables 7 and 8 of WSRC-STI-2008-00244). Jintan is located at a similar latitude to the SDF (approximately 31.722° N versus 33.305° degrees N). Jintan is approximately 30 miles from a major river (the Yangtze to the north) and approximately 100 miles from the east coast of mainland China. The SDF is located approximately 10 miles from a major river (the Savannah River) and approximately 90 miles from the east coast of South Carolina. These general similarities suggest that the 3,000-year-old burial mounds of the Tu-Dun tombs (Figure 4.3-2) provide a reasonable analog for postulating the long-term performance of man-made earthen structures similar to the SDF closure cap.

Figure 4.3-1: Analog Site: 8-Year-Old Engineered Cover in Omaha, NE

[ML12005A110, SRRA107772-000009, Figure 3.2-37 of SRR-CWDA-2019-00001]

Figure 4.3-2: Analog Site: 3,000-Year-Old Tu-Dun Tombs in South-Central China

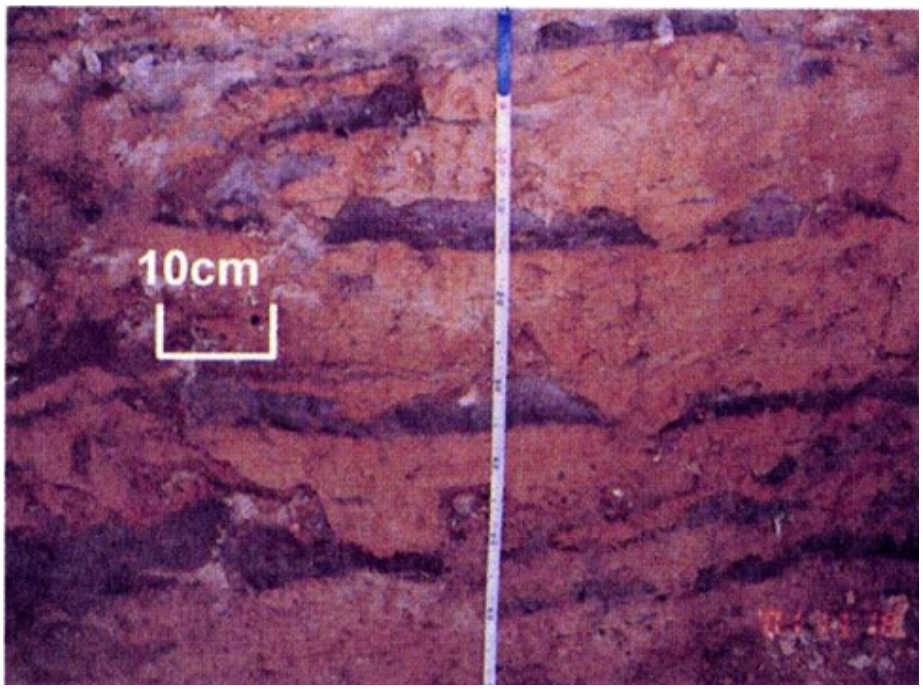

[Onitsuka, et.al. (2006), SRRA107772-000009, Figure 3.2-38 of SRR-CWDA-2019-00001]

Figure 4.3-3: Analog Site: 2,000-Year-Old Burial Mound in Northern Kyushu Prefecture, Japan

[Hudson and Barnes (1991), SRRA107772-000009, Figure 3.2-39 of SRR-CWDA-2019-00001]

4.3.2 Other Observations Suggesting that Silting-In Will Not Occur

Despite the similarities between SRS and the Tu-Dun site described in Section 4.3.1, the site was not constructed with the exact same design (or materials) as the SDF closure cap. Therefore, there remains some uncertainty relative to the applicability of this site as an analog for SRS closure caps.

Additionally, *Engineered Covers for Waste Containment: Changes in Engineering Properties and Implications for Long-Term Performance Assessment, Vol. 1* (NUREG/CR-7028 [ML12005A110]) indicated that "[d]ownward percolation of pore water containing Ca and Mg from overlying cover soils is generally cited as a source of divalent cation exchange." However, it should be noted that the downward migration of ions dissolved in pore water is not necessarily indicative of the downward migration of mineral solids. The ions in pore water are from soluble salts on the mineral surfaces, which enter the profile during infiltration and later precipitate on the solid surfaces. They are mobilized again as infiltrating water migrates downward in the profile, but this is not indicative of movement of mineral solids at the macroscopic or molecular levels (Benson, 2021).

NUREG/CR-7028 also described observations of exhumed closure caps where "[m]odest amounts of soil were present in many of the geotextiles and the geonets contained a coating of fines in some cases." Although this observation was limited to the geotextile and geonet fabrics that separate the different soil materials (i.e., a potential barrier to further downward migration), the observation can be interpreted as indicating that fine grained materials will eventually mobilize and move into lower layers. However, Dr. Craig Benson, one of the authors of NUREG/CR-7028 [ML12005A110], has expressed concerns with respect to assuming this is phenomenon (Benson, 2021). He believes that this is:

> "a hypothetical issue, which is not supported by observed [conditions] in engineered cover systems or natural analogs. In contrasts [*stet*] to aqueous systems or fluvial environments, the pore water in cover systems has too little energy (e.g., in terms of pressure) to induce migration of fines into a drainage layer provided that proper filter criteria have been followed during design and construction" (Benson 2021).

and:

> "[T]he presence or accumulation of fines on the surface of geotextiles or directly above a coarse earthen layer is common and expected, but is not indicative of 'silting in' that might occur in a fluvial environment with higher energy. The finer particles that accumulate at the interface with a sand drainage layer or a geotextile form bridges across the larger pores in the coarser material below, creating a thin 'filter' layer directly above the drainage layer. This filter mechanism keeps the underlying drainage material free of fines." (Benson, 2021).

Regardless, although the process of silting-in is not considered likely, it remains plausible such that further consideration is warranted as a pessimistic postulation. Until the phenomenon can be further investigated and ruled-out, it is recommended that probabilistic modeling apply silting-in as an assumed degradation mechanism.

4.3.3 Modeling Parameters Needed to Address the Possibility of Silting-In

If sand degradation via the silting-in process is assumed to occur, it is expected to occur as a gradual process, and to be completed once the K_{sat} of the upper sand drainage layer reaches an equilibrium end state. Since a degraded closure cap of the same conceptual design as the SDF closure cap does not exist, this equilibrium end state is unknown. It is assumed that the equilibrium state will be a final sand K_{sat} value that is lower than the initial sand K_{sat}, and higher than or equal to the K_{sat} of the overlying backfill.

Based on this assumption, the K_{sat} for the backfill is needed to estimate the lower bound of the end state value. The mean backfill K_{sat} (4.1E-05 cm/s) is from Table 5-18 of WSRC-STI-2006-00198. The assumed minimum and maximum values are from Section 5.8.3.2 of the 2019 SDF PA (SRR-CWDA-2019-00001) and were developed by modifying the generically recommended minimum and maximum values from Section 10.2 of NUREG/CR-7028 (ML12005A110). NUREG/CR-7028 recommended a minimum of 1.0E-05 cm/s, so using our site-specific value of 4.1E-05 cm/s, the minimum was assumed to be the geometric mean of the site-specific mean and the recommended minimum: GEOMEAN(4.1E-05, 1.0E-05) = 2.0E-05 cm/s. Similarly, NUREG/CR-7028 recommended a maximum of 5.0E-04 cm/s, so the maximum was assumed to be the geometric mean of the site-specific mean and the recommended maximum: GEOMEAN(4.1E-05, 5.0E-04) = 1.4E-04 cm/s.

Next, based on the textural triangle from WSRC-STI-2006-00198 (Figure 5-29), shown here as Figure 4.3-4, the backfill material is generally expected to be a sandy clay loam. Table A-4 of NUREG/CR-6565 recommends using a log-normal distribution for estimating the K_{sat} of a generic sandy clay loam.

Figure 4.3-4: Textural Triangle for Controlled Compacted Backfill (Fig. 5-29 from WSRC-STI-2006-00198)

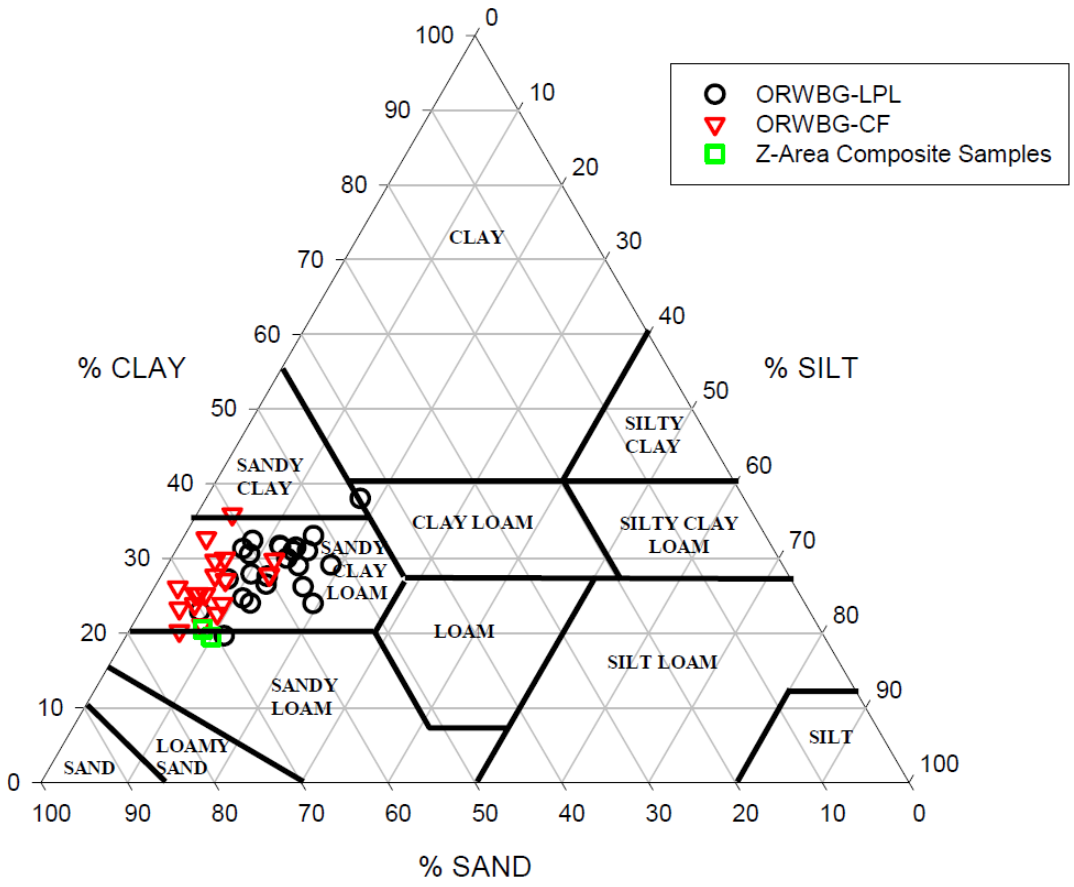

ORWBG-LPL = Old Radioactive Waste Burial Ground – Low Permeability Layer
ORWBG-CF = Old Radioactive Waste Burial Ground – Common Fill

For the standard deviation, the value of 5.98E-04 cm/s (from Table A-4 of NUREG/CR-6565) was scaled down by applying a factor of 0.127 (to 7.59E-05 cm/s) because the assumed mean of 4.10E-05 cm/s is approximately 0.127 times the mean recommended for the generic sandy clay loams (3.23E-04 cm/s from Table A-4 of NUREG/CR-6565). These recommendations are summarized in Table 4.3-1 and Figure 4.3-5 shows the resulting probability density function. As with the initial sand distribution, the distribution for the backfill K_{sat} is also skewed towards selecting lower values.

Table 4.3-1: Recommended Distribution for Modeling Backfill K_{sat}

Distribution Parameter	Generic Sandy Clay Loam K_{sat} (cm/s) per NUREG/CR-6565	Recommendation for K_{sat} (cm/s) Backfill	Basis for Backfill Recommendations
Mean	3.23E-04	4.10E-05	Recommended vertical saturated hydraulic conductivity of controlled compacted backfill at SRS from Table 5-18 of WSRC-STI-2006-00198
Standard Deviation	5.98E-04	7.59E-05	Because the assumed mean (4.1E-05 cm/s) is 7.88 times lower than the mean in Table A-4 of NUREG/CR-6565 (5.98E-04 cm/s), the standard deviation was scaled down by the same factor: 5.98E-04/7.88 = 7.59E-05
Minimum	4.12E-07	2.0E-05	From Section 5.8.3.2 of the 2019 SDF PA (SRR-CWDA-2019-00001)
Maximum	2.02E-02	1.4E-04	From Section 5.8.3.2 of the 2019 SDF PA (SRR-CWDA-2019-00001)
Shape	Log-Normal		Generic Sandy Clay Loam Distribution from Table A-4 of NUREG/CR-6565

Figure 4.3-5: Probability Density Function for the Recommended Backfill K_{sat}

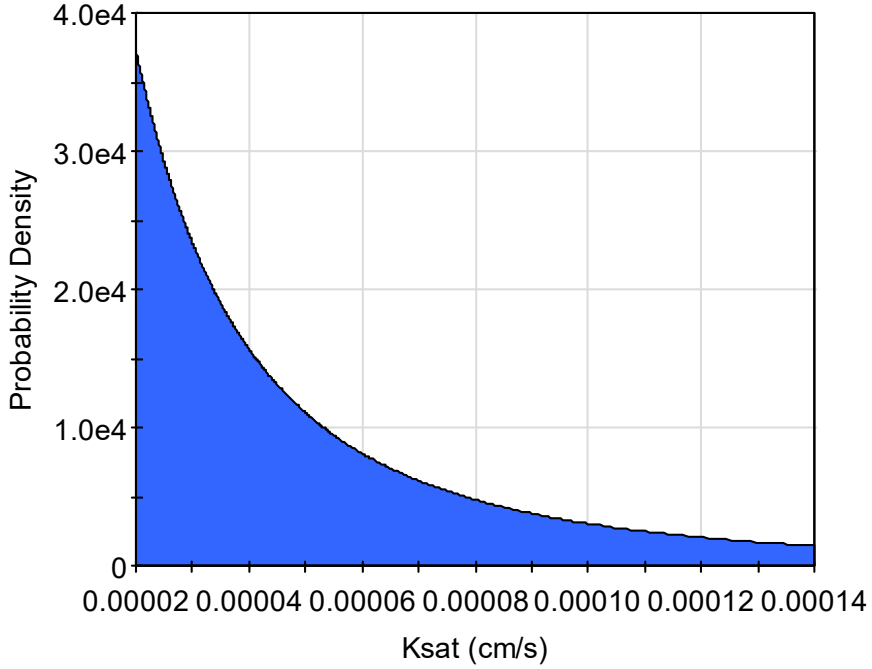

Note that the backfill mean (4.1E-05 cm/s) from Table 4.3-1 represents the vertical K_{sat} of the backfill. The vertical K_{sat} is used because it is assumed that the predominant direction of flow from the backfill into the sand will be downward. However, once the clays (or other fine particles) migrate from the backfill into the coarse sand, the predominant direction of flow is expected to be

lateral. Because the horizontal K_{sat} of the backfill is nearly twice as high (7.6E-05 cm/s per Table 5-18 of WSRC-STI-2006-00198), the use of the lower value is expected to yield slightly conservative results.

Since the final degraded state of the sand is unknown, the initial sand K_{sat} and the backfill K_{sat} values can be used as the upper and lower bounds, respectively, for sampling on a log-triangular distribution to estimate the final, degraded sand K_{sat} (Table 4.3-2 and Figure 4.3-6).

Table 4.3-2: Recommended Final Sand K_{sat} Distribution for Modeling Upper and Lower Lateral Sand Drainage Layers

Distribution Parameter	Recommendation for K_{sat} (cm/s) of Degraded Sand in the Upper and Lower Lateral Sand Drainage Layers	Basis for Upper and Lower Lateral Sand Drainage Layers Recommendations
Minimum	Sampled backfill K_{sat} from Table 4.3-1	Since degradation is attributed to clays and fines migrating from the overlying backfill into the coarse sand layer, it is assumed that the backfill K_{sat} provides the lower bound of the final degraded state.
Mode	One order of magnitude less than the sampled initial sand K_{sat} from Table 3.2-2	Since the analog sites discussed in Section 4.3.1 suggest that silting-in is unlikely to occur, it is not appropriate to assume that the mode of the final degraded state is directly associated with backfill. Given the time periods being considered it is also not appropriate to assume a final end state in which the sand K_{sat} remains fully un-impacted. Therefore, for the mode, it is assumed that the K_{sat} will decrease by a full order of magnitude. Thus, in the log-triangular distribution the selected mode lies about a third of the way between the initial sand and backfill conductivity values, modestly biased toward the expected long-term condition compared to the midpoint.
Maximum	Sampled initial sand K_{sat} from Table 3.2-2	Since the analog sites discussed in Section 4.3.1 suggest that silting-in might not occur, it is appropriate to assume the initial sand K_{sat} for both the mode and the upper bound of the final degraded state.
Shape	Log-Triangular	The selection of the distribution shape was limited because there is insufficient information about long-term sand performance. When the only information known about a parameter is the range (minimum and maximum values), then a uniform or log-uniform distribution is most appropriate. However, in the case of this distribution, it is appropriate to assume a triangular distribution because it is expected that the silting-in phenomenon is unlikely to occur to a significant extent. As a result, this sampling distribution is skewed to the right (as shown in Figure 4.3-6). The log-triangular was selected over the triangular distribution because the log-triangular distribution samples lower sand K_{sat} values more often than the triangular distribution. The resulting probability density function (Figure 4.3-6) has a peak near 1.0E-04 cm/s, which is near the mean K_{sat} for sampling a Generic Sandy Clay Loam Distribution from Table A-4 of NUREG/CR-6565. This suggests that the selected parameters may result in an end state in which the coarse sand

		evolves into the approximate equivalent of a typical sandy clay loam.

Figure 4.3-6: Probability Density Function for the Final Sand K_{sat}

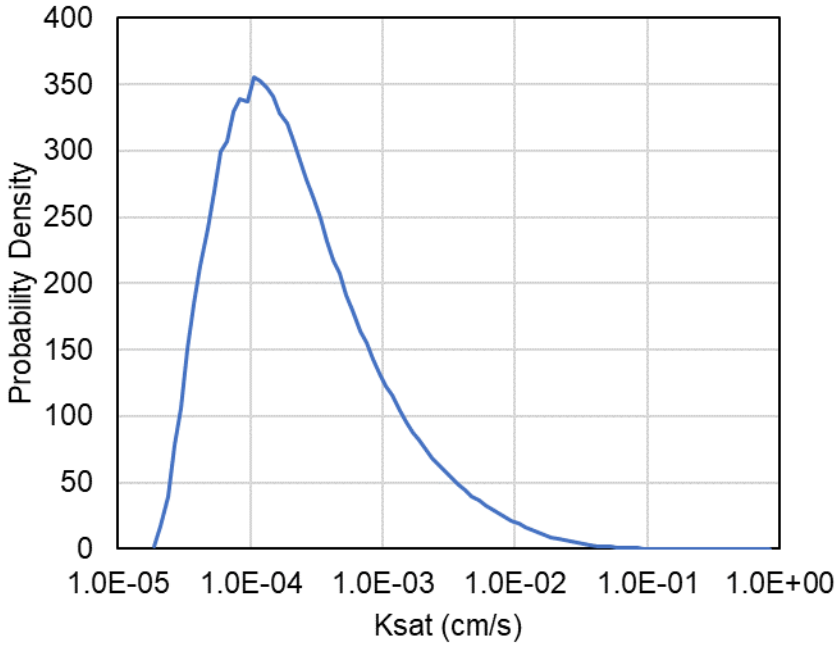

Note: Because this distribution relies on the sampling results of two other distributions, this probability density was developed from the results from 1,000,000 samples. The "uneven" appearance near the peak is attributed to the histogram probability density intervals selected during the development the figure.

Next, assumptions are needed to determine how long it would take for the silting-in process to fully degrade the sand. A similar closure cap concept report, *FTF [6]Closure Cap Concept and Infiltration Estimates* (WSRC-STI-2007-00184), postulated a rate of 10 inches per 5,000 years based on formation of B-horizons from the deposition of translocated clay. Using this assumption, it would take 6,000 years for 100% of the fines to migrate from the backfill into the upper sand drainage layer. However, as indicated in Appendix I of WSRC-STI-2007-00184, it is assumed that once half of the fines content of the backfill has migrated to the drainage layer, the two layers essentially become the same material, so only 50% of the fines are needed to reach equilibrium. Therefore, the silting-in degradation process is assumed to take half as long (3,000 years).

For uncertainty, a log-triangular distribution is assumed, where the minimum time is 300 years, the mode is 3,000 years, and the maximum time is 30,000 years (i.e., ± an order of magnitude). This very wide range is reasonable given that no field information is available as to how long such a process may actually take to occur and, if it does occur, this process is expected to be slow; alternatively, the shape of the assumed distribution is conservative because applying the triangular log distribution skews the sampling to preferentially select earlier years, resulting in faster degradation rates. This distribution is summarized in Table 4.3-3 and shown in Figure 4.3-7.

[6] FTF = F-Area Tank Farm

With each of the sampling parameters defined, the evolution of the sand K_{sat} can be determined (see Section 5.0).

Table 4.3-3: Recommended Distribution for Modeling the Time Required for Complete Sand Degradation via Silting-In in the Upper Lateral Drainage Layer

Distribution Parameter	Years	Basis for Backfill Recommendations
Minimum	300	1/10th of the Mode
Mode	3,000	Based on recommendation in WSRC-STI-2007-00184
Maximum	30,000	10 times the Mode
Shape	Log-Triangular	Generic Sandy Clay Loam Distribution from Table A-4 of NUREG/CR-6565

Figure 4.3-7: Probability Density Function for the Time to Complete Sand Degradation via Silting-In

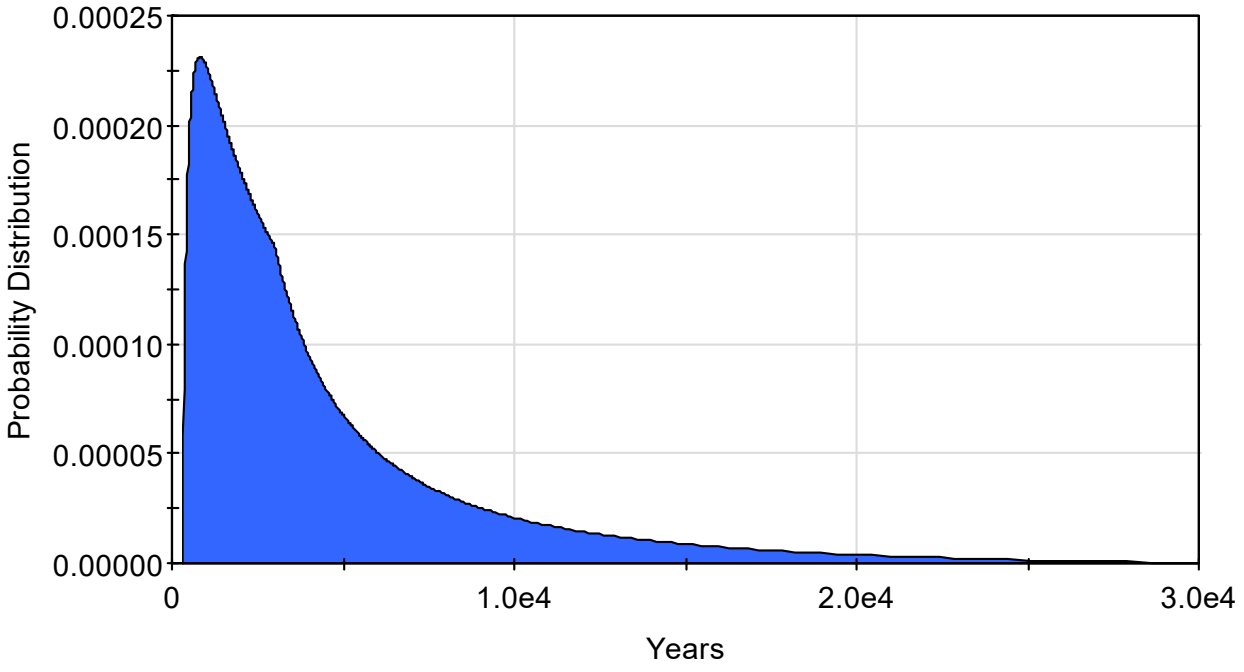

5.0 ESTIMATED EVOLUTION OF SAND K_{sat} VALUES

When estimating the long-term evolution of the sand K_{sat}, there are multiple parameters to consider, as were discussed in Sections 3.0 and 4.0. Section 5.1 describes how to implement these recommended parameters to simulate the evolution of the sand K_{sat} in the upper lateral drainage layer and Section 5.2 describes how to simulate the evolution of the sand K_{sat} in the lower lateral drainage layer.

5.1 Sand K_{sat} Evolution in the Upper Lateral Drainage Layer

Once the initial sand K_{sat} (Table 3.2-2) and the backfill K_{sat} values have been sampled (Table 4.3-1), the final degraded sand K_{sat} (Table 4.3-2) may be sampled. These values, along with the sampled time required to complete sand degradation (Table 4.3-3) may be used to simulate the long-term evolution of the sand K_{sat} in the upper lateral drainage layer of the SDF closure cap in a way that appropriately accounts for uncertainties.

If the elapsed time (t) in the model is less than the sampled time to complete sand degradation via silting-in (t_{sand}^{deg}) (Table 4.3-3), then an intermediate value for the saturated hydraulic conductivity of the sand ($K_{sat,t}$) may be estimated as

$$K_{sat,t} = 10^{\left[\log(K_{sat}Final)\times\left(\frac{t}{t_{sand}^{deg}}\right)+\log(K_{sat}Initial)\times\left(1-\frac{t}{t_{sand}^{deg}}\right)\right]} \times F_{(root)}$$

where $K_{sat,t}$ is the intermediate sand K_{sat} (cm/s) at time = t,

$K_{sat}Final$ is the end state for the sand in cm/s based on Table 4.3-3,

$K_{sat}Initial$ is the initial state for the sand K_{sat} in cm/s based on Table 3.2-2,

t is the simulation time (yr),

t_{sand}^{deg} is the sampled time to complete sand degradation via silting-in based on Table 4.3-3, and

$F_{(root)}$ is the root function multiplier (0.998) from Section 4.2.

This approach is based on Appendix I of WSRC-STI-2007-00184 (i.e., the 2007 closure cap report for the FTF), which varies slightly from a similar approach described in Appendix I of WSRC-STI-2008-00244 (i.e., the 2008 closure cap report for the SDF). The 2007 report applied a logarithmic rate of change that is initially fast, but gradually slows down as the lateral drainage layer approaches the end state, while the 2008 report applied a constant (linear) rate of change. By applying the approach from WSRC-STI-2007-00184, significant degradation occurs much earlier.

Finally, if the simulated time (t) in the model is greater than the sampled time to complete sand degradation via silting-in (t_{sand}^{deg}), then $K_{sat}Final$ times the root function multiplier (0.998) is used.

5.2 Sand K_{sat} Evolution in the Lower Lateral Drainage Layer

The lower lateral drainage layer is two feet thick, which is twice as thick as the upper lateral drainage layer, and it is buried deeper within the closure cap. As such, it is appropriate to assume

that the sand in the lower later drainage layer will take longer to undergo complete degradation. Therefore, it is assumed to take twice as long to fully degrade ($t_{sand}^{deg} \times 2$).

Further, because the lower lateral drainage layer is deeper, and below the impervious HDPE geomembrane, it is expected to be beyond the rooting depth, such that the root function multiplier is not applicable.

Accordingly, if the simulated time (t) in the model is less than twice the sampled time to complete sand degradation via silting-in ($t_{sand}^{deg} \times 2$), the intermediate value for the saturated hydraulic conductivity of the sand ($K_{sat,t}$) may be estimated as

$$K_{sat,t} = 10^{\left[\log(K_{sat}Final)\times\left(\frac{t}{t_{sand}^{deg}\times 2}\right)+\log(K_{sat}Initial)\times\left(1-\frac{t}{t_{sand}^{deg}\times 2}\right)\right]}$$

where $K_{sat,t}$ is the intermediate sand K_{sat} (cm/s) at time = t,

$K_{sat}Final$ is the end state for the sand in cm/s based on Table 4.3-3,

$K_{sat}Initial$ is the initial state for the sand K_{sat} in cm/s based on Table 3.2-2,

t is the simulation time (yr), and

t_{sand}^{deg} is the sampled time to complete sand degradation via silting-in based on Table 4.3-3.

Finally, if the simulated time (t) in the model is greater than twice the sampled time to complete sand degradation via silting-in ($t_{sand}^{deg} \times 2$), then $K_{sat}Initial$ is used.

6.0 RESULTS

The sampling distributions and calculations defined throughout this report were applied to a probabilistic model using GoldSim modeling software. The model was run for a simulated duration of 10,000 years and applied for 1,000 realizations. Sections 6.1 and 6.2 provide the results for the upper lateral drainage layer and the lower lateral drainage layer, respectively.

6.1 Simulation Results for the Sand K_{sat} Evolution in the Upper Lateral Drainage Layer

Table 6.1-1 provides a summary of the estimated values for the upper lateral drainage layer at selected times. Figure 6.1-1 shows the resulting probability time history over 10,000 years. Relative to the data from Hwang et al. (2017), shown in Table 3.2-1, these values indicate that the typical evolution is for the sand to evolve from coarse grained to fine grained, with extreme conditions that vary from the sand remaining relatively unchanged to the sand evolving into backfill material. The assumed SDF PA conductivities are less than the mean value of the stochastic distribution for all times and less than the 25th percentile through 1,000 years.

Table 6.1-1: Summary of Estimated Sand K_{sat} at Selected Times (for the Upper Lateral Drainage Layer)

Statistic	K_{sat} (cm/s) at t = 0 yrs	K_{sat} (cm/s) at t = 100 yrs	K_{sat} (cm/s) at t = 1,000 yrs	K_{sat} (cm/s) at t = 10,000 yrs
Maximum	6.87E-01	6.00E-01	4.67E-01	2.38E-01
95th %	3.08E-01	2.67E-01	1.65E-01	5.91E-02
75th %	1.89E-01	1.60E-01	8.00E-02	1.67E-02
Median	1.30E-01	1.11E-01	4.38E-02	6.13E-03
25th %	8.96E-02	7.49E-02	1.55E-02	1.43E-03
5th %	6.05E-02	4.85E-02	1.33E-03	1.844E-04
Minimum	5.04E-02	2.25E-02	1.08E-04	2.59E-05
Mean	1.50E-01	1.28E-01	5.73E-02	1.47E-2
Value used in 2019 SDF PA (SRR-CWDA-2019-00001)[a]	5.00E-02	5.00E-02	1.00E-02	1.00E-02

Note: [a] Compliance Case value changes from 5.00E-02 cm/s to 1.00E-02 cm/s as an assumed step change at 500 years.

Figure 6.1-1: Estimated Sand K_{sat} in the Upper Lateral Drainage Layer Based on Sampling Recommendations

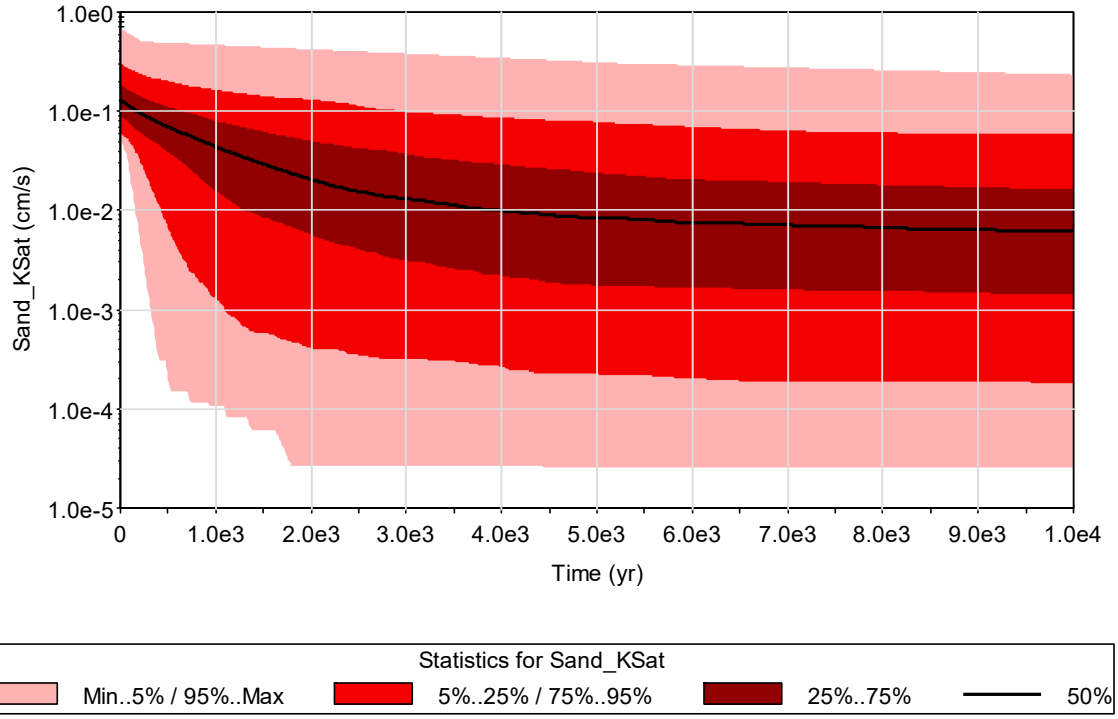

6.2 Simulation Results for the Sand K_{sat} Evolution in the Lower Lateral Drainage Layer

Table 6.2-1 provides a summary of the estimated values for the lower lateral drainage layer at selected times. Figure 6.2-1 shows the resulting probability time history over 10,000 years. Again, the assumed SDF PA conductivities are less than the mean value of the stochastic distribution for all times and less than the 25th percentile through 1,000 years.

Table 6.2-1: Summary of Estimated Sand K_{sat} at Selected Times (for the Lower Lateral Drainage Layer)

Statistic	K_{sat} (cm/s) at t = 0 yrs	K_{sat} (cm/s) at t = 100 yrs	K_{sat} (cm/s) at t = 1,000 yrs	K_{sat} (cm/s) at t = 10,000 yrs
Maximum	6.89E-01	6.43E-01	4.92E-01	3.13E-01
95th %	3.09E-01	2.82E-01	2.03E-01	7.85E-02
75th %	1.89E-01	1.73E-01	1.12E-01	2.40E-02
Median	1.30E-01	1.21E-01	6.98E-02	8.40E-03
25th %	8.98E-02	8.29E-02	3.88E-02	1.77E-03
5th %	6.06E-02	5.47E-02	6.67E-03	2.25E-04
Minimum	5.05E-02	3.87E-02	2.03E-04	2.60E-05
Mean	1.50E-01	1.38E-01	8.22E-02	1.97E-02
Value used in 2019 SDF PA (SRR-CWDA-2019-00001) [a]	5.00E-02	5.00E-02	1.00E-02	1.00E-02

Note: [a] Compliance Case value changes from 5.00E-02 cm/s to 1.00E-02 cm/s as an assumed step change at 500 years.

Figure 6.2-1: Estimated Sand K_{sat} in the Lower Lateral Drainage Layer Based on Sampling Recommendations

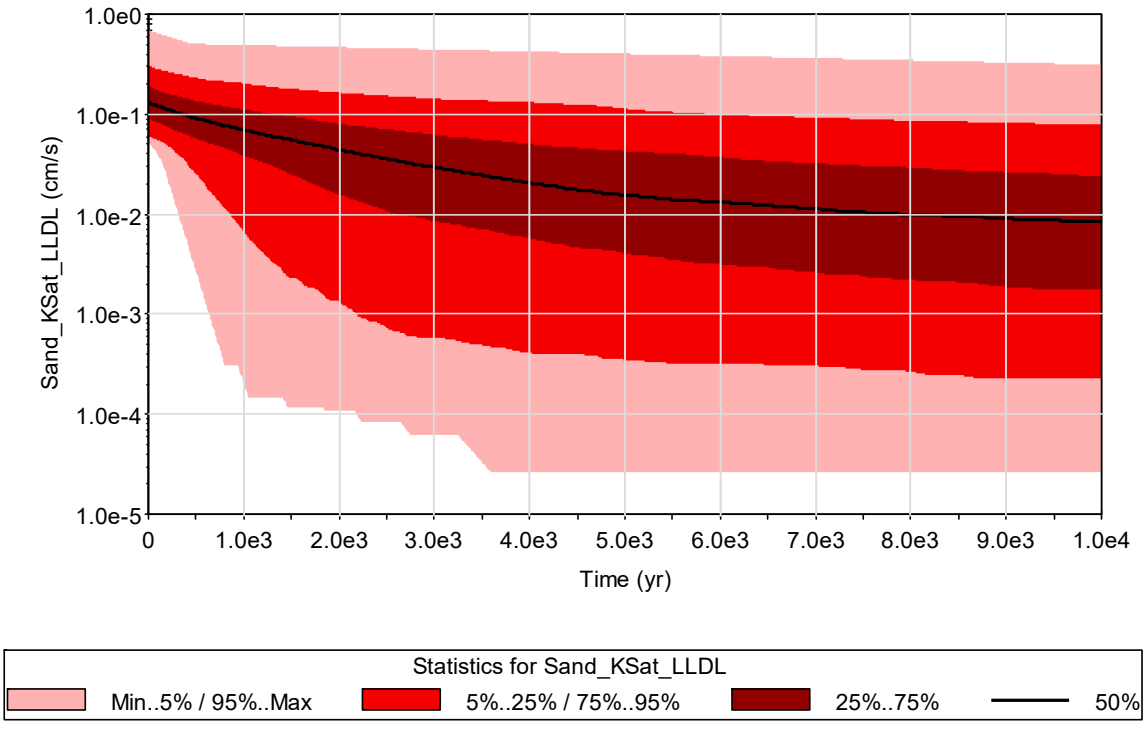

This page intentionally left blank.

7.0 REFERENCES

Bear, J. (1972). See ISBN 13:9780486656755.

Benson, C.H. (2021). Personal communication with Steven Hommel, March 13, 2021.

Benson, C.H. and Benavides, J.M. (2018). See SRRA107772-000009.

Brewer, C. W., (1975), *Rooting Depth of Mature Loblolly Pine (Pinus Taeda L.) as Influenced by Physical Properties of the Soil in Southeastern Louisiana*, LSU Historical Dissertations and Theses, 2863. https://digitalcommons.lsu.edu/gradschool_disstheses/2863

EPA/600/R-94/168b, Schroeder, P. R., Dozier, T. S., Zappi, P. A., McEnroe, B. M., Sjostrom, J. W., and Peyton, R. L., *The Hydrologic Evaluation of Landfill Performance (HELP) Engineering Documentation for Version 3*, Office of Research and Development, United States Environmental Protection Agency (EPA), Cincinnati, Ohio. September 1994.

Fetter, C. W. (1988). See ISBN 13: 9780675208871.

Freeze, R.A., and Cherry, J.A. (1979). See ISBN 13: 978-0133653120.

Giroud, J.P., *Equations for Calculating the Rate of Liquid Migration Through Composite Liners Due to Geomembrane Defects*, Geosynthetics International, Vol. 4, No. 3-4, January 1997. ISSN 1072-6349, (Copyright)

Giroud, J.P., et.al., *Liquid Flow Equations for Drainage Systems Composed of Two Layers Including a Geocomposite*, Geosynthetics International, Vol. 11, No. 1, February 2004. DOI: 10.1680/gein.2004.11.1.43 (Copyright)

Hillel, D. (1982). See ISBN: 9780123485205.

Hudson, M., and Barnes, G., *Yoshinogari: A Yayoi Settlement in Northern Kyushu*, Monumenta Nipponica, 46(2): 211-235, 1991. (Copyright)

Hwang, H., Jeen, S., Suleiman, A. and Lee, K., (2017), Comparison of Saturated Hydraulic Conductivity Estimated by Three Different Methods, Water, Vol. 9 (942), December 2017. DOI:10.3390/w9120942 (Copyright)

ISBN 13: 978-0133653120, Freeze, R.A., and Cherry, J.A., *Groundwater*, Prentice-Hall, Engelwood Cliffs, NJ, 1979. (Copyright)

ISBN 13: 9780675208871, Fetter, C. W., *Applied Hydrogeology*, 2nd edition. Macmillan Publishing Company, New York, 1988. (Copyright)

ISBN 13:9780123485205, Hillel, D., *Introduction to Soil Physics*, Academic Press, Inc., San Diego, CA, 1982. (Copyright)

ISBN: 13:9780471024910, Lamb, T. W. and Whitman, R. V., *Soil Mechanics*, John Wiley & Sons, New York, 1969. (Copyright)

ISBN: 9780486656755, Bear, J., *Dynamics of Fluids in Porous Media*, Elsevier Scientific, New York, 1972. (Reprinted by Dover, New York, 1988) (Copyright)

Jones and Phifer (2008). See WSRC-STI-2008-00244.

Lamb, T. W. and Whitman, R. V. (1969). See ISBN: 13:9780471024910.

ML091200509, (NUREG/CR-6565), Meyer, P.D., Rockhold, M.L., and Gee, G.W., *Uncertainty Analyses of Infiltration and Subsurface Flow and Transport for SDMP Sites*, Pacific Northwest National Laboratories for the U.S. Nuclear Regulatory Commission, Office of Nuclear Regulatory Research, Richland, WA, September 1997.

ML12005A110, (NUREG/CR-7028), Benson, C.H., et al., Engineered Covers for Waste Containment: Changes in Engineering Properties and Implications for Long-Term Performance Assessment, Vol. 1, U.S. Nuclear Regulatory Commission, Office of Nuclear Regulatory Research, Washington, December 2011.

ML20254A003, Koenick, S. S., *Preliminary Review of the U.S. Department of Energy's Submittal of the 2020 Savannah River Site Saltstone Disposal Facility Performance Assessment*, U.S. Nuclear Regulatory Commission, Office of Nuclear Regulatory Research, Washington, October 2020.

NUREG/CR-6565. See ML091200509.

NUREG/CR-7028. See ML12005A110.

Onitsuka, K., Lu, L., Tang, X., Hara, Y., and Kai, D., *Geotechnical Characteristics and Construction Methods of Yoshinogari Fun-Kyu Tomb in Japan and Tu-Dun Tombs in China*, Japan Society of Civil Engineers (J-STAGE), Vol. 2003 (736) pp. 1-17, June 2003. doi.org/10.2208/jscej.2003.736_1 (Copyright)

Phifer, et al. (2001). See WSRC-TR-2001-00015.

Phifer, et al. (2006). See WSRC-STI-2006-00198.

Phifer, et al. (2007). See WSRC-STI-2007-00184.

SCDHEC R.61-107.19, *SWM: Solid Waste Landfills and Structural Fill*, South Carolina Department of Health and Environmental Control, Columbia, SC, May 2008.

Schroeder, et al. (1994). See EPA/600/R-94-168b.

SRRA107772-000009, Benson, C.H., and Benavides, J.M., *Predicting Long-Term Percolation from the SDF Closure Cap*, Report No. GENV-18-05, University of Virginia School of Engineering, April 2018.

SRR-CWDA-2018-00006, *Conceptual Model Development for the Saltstone Disposal Facility Performance Assessment*, Savannah River Remediation, Aiken, SC, Rev. 0, May 2018.

SRR-CWDA-2018-00035, *Savannah River Site Salt Waste Disposal NRC Onsite Observation Visit July 9-11, 2018*, Savannah River Remediation, Aiken, SC, Rev. 0, May 2018.

SRR-CWDA-2018-00068, Watkins, D.R., *Performance Assessment for the Saltstone Disposal Facility at the Savannah River Site: Quality Assurance Report*, Savannah River Remediation, Aiken, SC, Rev. 2, January 2020.

SRR-CWDA-2018-00087, *Saltstone Disposal Facility Closure Cap Concept Update for Large-Scale Disposal Units*, Savannah River Remediation, Aiken, SC, Rev. 1, April 2019.

SRR-CWDA-2019-00001, *Performance Assessment for the Saltstone Disposal Facility at the Savannah River Site*, Savannah River Remediation, Aiken, SC, Rev. 0, March 2020.

SRR-CWDA-2019-00110, *Determination of the SDF Inventory through 9/30/2019*, Savannah River Remediation, Aiken, SC, Rev. 0, January 2020.

SRR-CWDA-2020-00005, *Closure Plan for the Z-Area Saltstone Disposal Facility*, Savannah River Remediation, Aiken, SC, Rev. 1, August 2020.

SRR-LWP-2009-00001, Chew, D.P., Hamm, B.A., and Wells, M.N., *Liquid Waste System Plan*, Savannah River Remediation, Aiken, SC, Rev. 21, January 2019.

Wentworth, C.K., *A Scale of Grade and Class Terms for Clastic Sediments*, The Journal of Geology, Vol. 30 (5), pp. 377-392, August 1922. doi:10.1086/622910 (Copyright)

Wikipedia, *Jintan District*, article last updated June 2020. Website accessed November 2020: https://en.wikipedia.org/wiki/Jintan_District

WSRC-RP-93-894, Yu, A. D., Langton, C. A., and Serrato, M. G., *Physical Properties Measurement Program*, Westinghouse Savannah River Company, Aiken, SC, Rev. 0, June 1993.

WSRC-STI-2006-00198, Phifer, M. A., Millings, M. R., and Flach, G. P., *Hydraulic Property Data Package for the E-Area and Z-Area Soils, Cementitious Materials, and Waste Zones*, Washington Savannah River Company, Aiken, SC, Rev. 0, September 2006.

WSRC-STI-2007-00184, Phifer, M.A., et al., *FTF Closure Cap Concept and Infiltration Estimates*, Westinghouse Savannah River Company, Aiken, SC, Rev. 2, October 2007.

WSRC-STI-2008-00244, Jones, W.E. and Phifer, M.A., *Saltstone Disposal Facility Closure Cap Concept and Infiltration Estimates*, Westinghouse Savannah River Company, Aiken, SC, Rev. 0, May 2008.

WSRC-TR-2001-00015, Phifer, M. A., Nichols, R. L., Sappington, F. C., Steimke, J. L., and Jones, W. E., *TNX GeoSiphon™ Summary Report*, Westinghouse Savannah River Company, Aiken, SC, Rev. 0, January 2001.

Yu, et al. (1993). See WSRC-RP-93-894.